

INFLUENCE OF EVAPORATING RATE ON TWO-PHASE EXPANSION IN THE PISTON EXPANDER WITH CYCLONE SEPARATOR

Weifeng WU^{*}, Qi WANG, Zhao ZHANG, Zhijun WU, Xiaotian YANG, Liangcong XU

School of Energy and Power Engineering, Xi'an Jiaotong University, Xi'an, Shaanxi, 710049, China

^{*} Corresponding author; E-mail: weifengwu@xjtu.edu.cn

The Trilateral Flash Cycle shows a greater potentiality in moderate to low grade heat utilization systems due to its potentiality of obtaining high exergy efficiency, compared to the conventional thermodynamic cycles such as the Organic Rankine Cycles and the Kalina Cycle. The main difference between the Trilateral Flash Cycle and the conventional thermodynamic cycles is that the superheated vapor expansion process is replaced by the two-phase expansion process. The two-phase expansion process actually consists of a flashing of the inlet stream into a vapor and a liquid phase. Most simulations assume an equilibrium model with an instantaneous flashing. Yet, the experiments of pool flashing indicate that there is a flash evaporating rate. The mechanism of this process still remains unclear. In this paper, the flash evaporating rate is introduced into the model of the two-phase expansion process in the reciprocating expander with a cyclone separator. As such, the obtained results reveal the influence of evaporating rate on the efficiency of the two-phase expander.

Key words: *Trilateral Flash Cycle, two-phase expansion, reciprocating expander, evaporating rate, efficiency*

1. Introduction

Nowadays, efficient utilization and conversion of energy has been a hot topic in the field of energy science. There are two types of typical and well-known thermodynamic cycles in the field of low to medium temperature waste heat recovery, namely the Organic Rankine Cycles (ORCs) [1-5] and the Kalina Cycle [6-11].

Recently, the Trilateral Flash Cycle (TFC) has attracted more and more interest because of its better matching of the temperature profiles in the heater and its greater potentiality of obtaining high exergy efficiency [12-15]. Several authors showed that the TFC could have a better performance than the traditional ORCs [16-18]. However, there are also some troublesome difficulties in the process of designing and operating of the TFC-system, and one of the main difficulties is the design of the expander with high volume expansion ratio [19]. To solve this problem, simulations and experiments of two-phase expanders were carried out. Both the reciprocating expanders and twin screw expanders were suggested as possible candidates [20, 21].

Hiroshi Kanno et al. [22] conducted an experiment study on the setup with cylinder and piston which mimics the reciprocating expander, and a model of two-phase adiabatic expansion in the reciprocating cylinder was also proposed in their study. The experimental data was used for model validation and the proposed model could reproduce the pressure evolution of the two-phase expansion

process within about 5% accuracy. Giuseppe Bianchi et al. [23] carried out numerical investigations of a two-phase twin-screw expander for the TFC applications and assessed the effects of inlet pressure, inlet quality and revolution speed on the expander performance.

However, little is known about the actual fundamentals of the two-phase expansion process. The isentropic efficiency of a two-phase expander was always assumed as a given value and was unknown in the published literature. For different structures, sizes and rotation speeds, efficiency of the two-phase expander would be different because of its altered leakage and flow resistance. Experiments conducted by Hiroshi Kanno et al. [24] showed that the efficiency of two-phase reciprocating expanders decreased with the increase of the piston speed. According to the experimental results, quasi-static process could not describe the real process of the two-phase expansion. It was believed that when the piston speed was increased, the lack of evaporation would result in the decrease of efficiency of the reciprocating expander. Therefore, it is crucial to include the evaporating rate in the simulation model and analyze the influence of the evaporating rate on the efficiency of the two-phase expander.

In this paper, the flash evaporating rate, which is the mass evaporated per unit of time and volume of the liquid, is introduced into the simulation model of the two-phase expansion process. The research is focused on a reciprocating expander with a cyclone separator. The obtained results show the influence of the evaporating rate on the two-phase expansion process.

2. The Evaporation Process and Evaporating Rate in the Cyclone

The flow diagram of the TFC with the reciprocating expander is shown in Fig. 1. The T-s diagram of the TFC is shown in Fig. 2.

To avoid the hydraulic shocks, injection and flash evaporation takes place in a small cyclone above the piston chamber. This cyclone provides the phase separation of liquid and vapor, keeps the liquid out of the piston chamber, and allows vapor flow into the cylinder. In this case, the flash evaporation occurs in the cyclone [25]. At the beginning of the expansion process, saturated liquid refrigerant is injected into the cyclone rapidly. When the piston moves, it results in a pressure decrease, which leads to supersaturation of the liquid. Then the liquid evaporates into vapor to fill the expanding cylinder. The evaporation of liquid refrigerant in the cyclone can be seen as the separation of liquid and vapor in a closed volume under decreasing pressure. During the expansion process, the liquid evaporates continuously under decreasing pressure. The driving force is the difference between the saturation pressure of the liquid and the inner pressure in the cyclone. Finally, the vapor expands in the reciprocating expander during the expansion process.

However, no literature of flash evaporation under these conditions is found by the authors. A similar topic in the field of desalination is superheated water exposed to a sudden pressure drop [26, 27]. Under a sudden pressure drop, the evaporating rate gradually decreases during time. In the two-phase expander, evaporation happens during all the working process. That means the pressure drop between the saturation pressure of the liquid and the inner pressure in the cyclone would be maintained at a constant or varying level during the working process. Because of such pressure drop, which is the driving force of evaporation, the evaporating rate might be maintained at corresponding level. Considering the condition that the pressure drop plays a major role in such superheated evaporation, the initial evaporating rate from water pools under such sudden pressure drop is suggested as the instantaneous evaporating rate during the two-phase expansion process. It is necessary to clarify that the evaporation processes of the water pool and the two-phase reciprocating expander are different,

however, this is the closest model that could be found. To get the closest evaporation model, the evaporation case in water pool for flowing water is adopted in this paper [28]. It is believed that such an evaporating rate would reveal its influence on the performance of the two-phase expander.

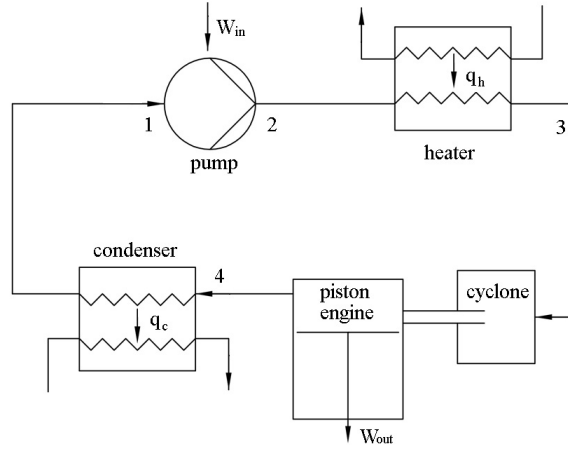


Fig. 1. Flow diagram of the TFC with piston expander and cyclone separator

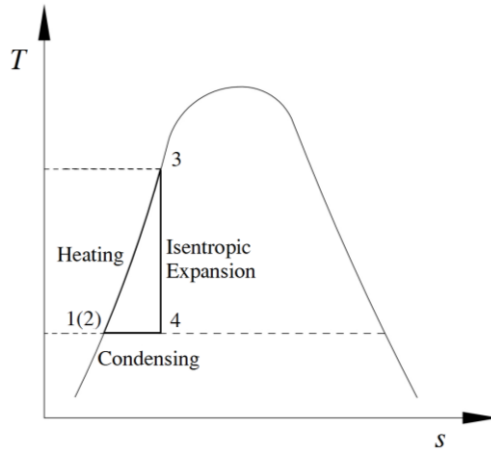


Fig. 2. The T-s diagram of the TFC with working fluid water

For the flash evaporation of water pools, where a sudden pressure drop would result in the superheat of the water film and result in its flash evaporation, a non-equilibrium function (NEF) was defined to describe the evaporation process [29], as shown in Eq. (1).

$$NEF(\tau) = \frac{T(t) - T_{sat}}{T_0 - T_{sat}} \quad (1)$$

Where T is the temperature of the superheated water, t is the time, T_{sat} is the saturation temperature of water under pressure p , T_0 is the initial temperature of the superheated water and τ is the dimensionless time for one stroke.

Evaporated mass during the evaporation process could be obtained based on Eq. (1) [30-33]. The evaporated mass, M_{ev} , is defined as Eq. (2).

$$M_{ev} = \frac{\rho c_p \Delta T}{r} [1 - NEF(\tau)] \quad (2)$$

Where ρ and c_p are density and isobaric heat capacity, respectively, ΔT is the degree of superheat, r is the latent heat of vaporization. One experiment reported the empirical formula of NEF [28], as shown in Eq. (3).

$$NEF(\tau) = erf \left[\left(\frac{H_0}{2} \sqrt{\frac{\rho c_p}{\mu t}} \right)^{a_2} \right] \quad (3)$$

Where H_0 is the height of the water film, μ and a_2 are expressed by Eq. (4) and Eq. (5), respectively.

$$\mu = 5.43 \times 10^3 \cdot H_0^{0.778} \cdot p^{0.558} \quad (4)$$

$$a_2 = 0.565 \cdot \Delta T^{0.181} \quad (5)$$

Then, the unit volume evaporating rate, m_{ev} [kg/m³], could be obtained from derivation of evaporated mass with respect to time, as shown in Eq. (6).

$$m_{ev} = \frac{a_2}{\sqrt{\pi}} \frac{\rho c_p \Delta T}{r} \left(\frac{H_0}{2} \sqrt{\frac{\rho c_p}{\mu}} \right)^{a_2} e^{-\left(\frac{H_0}{2} \sqrt{\frac{\rho c_p}{\mu}} \right)^{2a_2} t^{-a_2}} t^{-\frac{a_2+2}{2}} \quad (6)$$

For the water in the cyclone, the height, H_0 , could be replaced by the ratio of volume to the section area of the cyclone. Eq. (6) describes the evaporating rate along the time under local pressure p and the degree of superheat, ΔT . Obviously the initial evaporating rate is the maximum. This maximum evaporating rate, m_{mev} [kg/(m³·s)], is adopted to calculate the pressure evolution in the cylinder in this paper, as shown in Eq. (7).

$$m_{mev} = \frac{a_2}{\sqrt{\pi}} \rho c_p \left(\frac{V_L}{2A_0} \sqrt{\frac{\rho c_p}{\mu}} \right)^{a_2} \frac{\Delta T}{r} e^{-\left(\frac{V_L}{2A_0} \sqrt{\frac{\rho c_p}{\mu}} \right)^{2a_2} \tau_0^{-a_2}} \tau_0^{-\frac{a_2+2}{2}} \quad (7)$$

Where V_L is the volume of water in the cyclone, A_0 is the section area of the cyclone, and τ_0 is expressed by Eq. (8).

$$\tau_0 = \left(\frac{2a_2}{2+a_2} \right)^{\frac{1}{a_2}} \frac{V_L^2}{4A_0^2} \frac{\rho c_p}{\mu} \quad (8)$$

The experiment range of above evaporating rate is following: $1.5 \text{ K} \leq \Delta T \leq 48 \text{ K}$, $0.0003 \text{ m}^3 \leq V_L \leq 0.005 \text{ m}^3$, and its initial temperature range is $317 \text{ K} \leq T_0 \leq 368 \text{ K}$. This low temperature results in saturation pressure below atmospheric pressure. However, actual expanders typically work at higher pressure. Therefore, the initial temperature in this paper is set to 460 K. This arrangement is reasonable, because the temperature is not included in Eq. (7).

3. Model of the Expansion Process

The element evaporated mass is given by Eq. (9).

$$dM = V_L m_{mev} dt \quad (9)$$

Density of the liquid is assumed as constant during the process, thus evaporated volume of the water is shown as Eq. (10).

$$dV_L = \frac{1}{\rho} dM \quad (10)$$

To establish the simulation model, following assumptions are set.

(1) Walls of the expander and the cyclone are adiabatic.

This assumption is reasonable when insulation is applied in the expander, and rotation speed of the expander is fast.

(2) Water flow resistance in the cyclone and vapor flow resistance in the expander is ignored because it has no influence on vapor expansion in the cylinder.

(3) The latest evaporated vapor keeps its temperature at the saturation point.

(4) Latent heat of vaporization comes from the sensible heat of the water temperature decreasing.

(5) The vapor does isentropic expansion in the cylinder.

(6) The water in the cyclone does not expand.

(7) For the evaporated vapor, it flows into the cylinder, and then it is kept away from the water. It means there is no heat exchange between the vapor and the water in the cyclone.

Then the energy balance equation is obtained, as shown in Eq. (11).

$$Mdh_L = r dM \quad (11)$$

Based on Eq. (11), the temperature of the water in the cyclone could be obtained according to its enthalpy. For vapor, volume of new generated vapor is calculated by Eq. (12).

$$dV_v = \frac{dM}{\rho_v} \quad (12)$$

Based on the assumption of isentropic expansion, density of the vapor, ρ_v , could be obtained by giving the pressure and the initial entropy.

Time iteration method is adopted in the simulation program. Giving the time step, the new cylinder volume, V_c , could be obtained according to the piston motion. For a reciprocating expander, the equation of the piston motion and the volume of the cylinder are well known. Under the given time step, guessing a new pressure, the total volume, V_{total} , of vapor and liquid water could be obtained. Comparing the total volume, V_{total} , with the cylinder volume, V_c , if $V_{total} < V_c$, take a new smaller guessing value of pressure. If $V_{total} > V_c$, take a new bigger guessing value of pressure. When the difference between V_{total} and V_c is so tiny that it is less than the preset permission error e , the pressure should be the vapor pressure in the cylinder at this time step. Step by step, the pressure evolution process in the cylinder could be obtained. All thermal physic characteristics of water are obtained from the NIST Database [34]. The flowchart of the proposed time iteration algorithm is shown in Fig. 3.

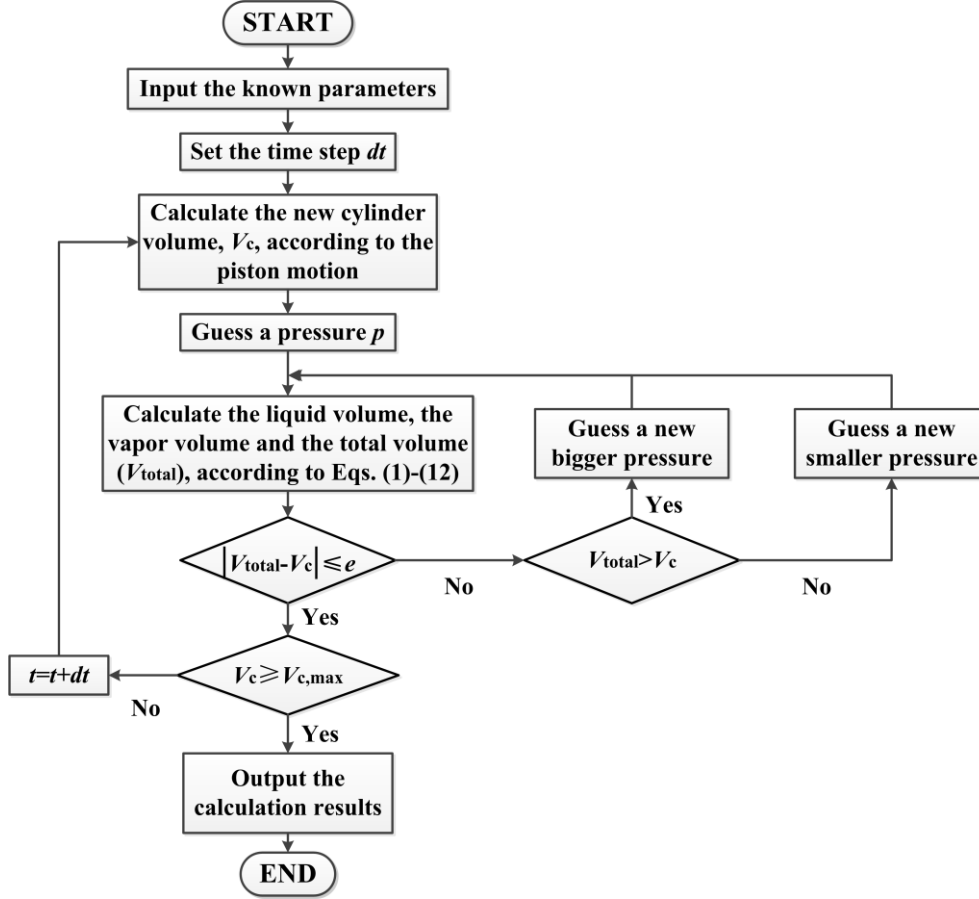


Fig. 3. Flowchart of the proposed time iteration algorithm

Outputted work of the expander is calculated by Eq. (13).

$$W = \int p dV_c \quad (13)$$

Thermal efficiency of the TFC can be obtained, as shown in Eq. (14).

$$\eta_{is-th} = \frac{60P}{M_0(h_3 - h_2)n} \quad (14)$$

Where P is the output power of the expander, h_3 and h_2 are the specific enthalpies of water at state points 3 and 2, respectively, n is the rotation speed of the expander, and M_0 is the initial mass of the water in the cyclone.

The isentropic efficiency of the expander, η_{is} , is defined as the ratio of outputted work to the isentropic work during two-phase expansion, as shown in Eq. (15).

$$\eta_{is} = \frac{60P}{M_0(h_3 - h_4)n} \quad (15)$$

4. Results and Discussion

The injected water is assumed at its saturated state. Thus the initial pressure in the cylinder is the saturation pressure. The volume of the cyclone (dead volume of the cylinder), the volume of cylinder, the injected mass, the initial temperature and the rotation speed of the expander will all influence the isentropic efficiency. To make sure the liquid is kept in the cyclone, the cyclone volume must be bigger than the initial volume of injected water, its ratio is defined as Eq. (16).

$$\delta = \frac{V_d}{M_i / \rho_L(T_0)} \quad (16)$$

Where, V_d is the cyclone volume, M_i is the injected mass of water, $\rho_L(T_0)$ is the density of water at initial temperature. The cyclone volume can also be seen as part of the dead volume in a reciprocating expander, the ratio of the dead volume to the cylinder volume is defined as Eq. (17).

$$\gamma = \frac{V_d}{V_c} \quad (17)$$

The shape of the cylinder is described by a ratio of its diameter to the stroke length, as shown in Eq. (18).

$$\lambda = \frac{d_c}{L} \quad (18)$$

Injected mass of the water is an important parameter. To evaluate this influence, a volume ratio, β , is defined as Eq. (19) and is the ratio of the saturated vapor volume at the initial temperature to the total volume of the expander. In addition, the pressure ratio, ε , that is the ratio of initial pressure p_0 to discharge pressure p_{dis} , is also considered as an important parameter which could evaluate whether the selection of operating parameters of the expander is reasonable, as shown in Eq. (20).

$$\beta = \frac{M_i / \rho_{v,sat}(T_0)}{V_c + V_d} \quad (19)$$

$$\varepsilon = \frac{p_0}{p_{dis}} \quad (20)$$

Table 1. Dimensionless ratios used in the present simulation

Ratio	Property	Function
τ	time ratio	to reflect the progress of the two-phase expansion under a stroke
δ	volume ratio	to determine the size of the cyclone volume
γ	volume ratio	to describe the relative size of the cyclone volume
λ	length ratio	to reflect the shape of the expander cylinder
β	volume ratio	to analyze the effect of the injected liquid mass
ε	pressure ratio	to evaluate whether the selection of operating parameters of the expander is reasonable

To conveniently analyze the influence of the operating parameters on the two-phase expansion process and clearly present the obtained results, it is very necessary to sum up all the dimensionless ratios above-defined in a separate table, as shown in Table 1.

4.1. Influence of the rotation speed

Among these parameters, influence from the rotation speed is primary. Pressure evolution profiles in the expander at different rotation speeds are shown in Fig. 4.

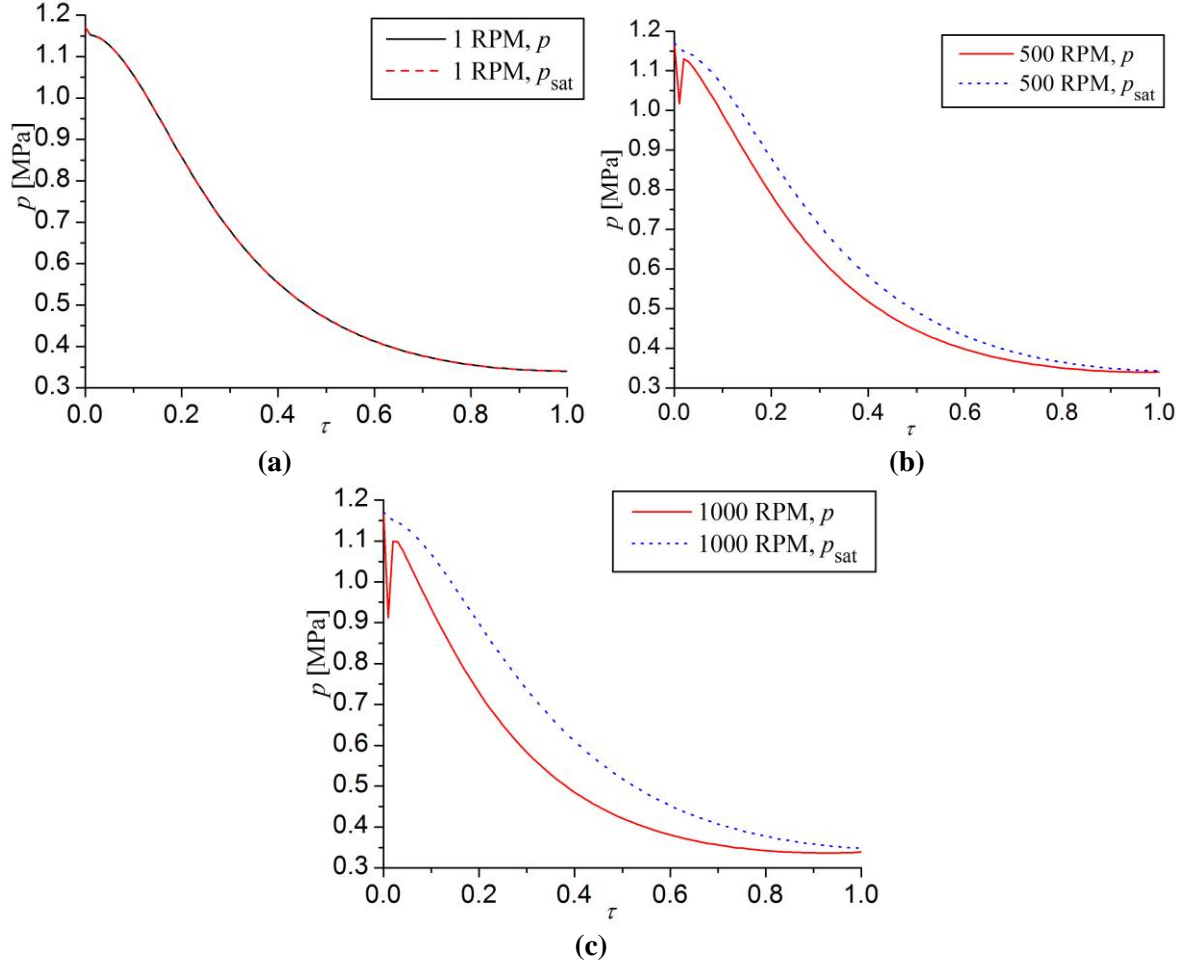


Fig. 4. Pressure evolution profiles during the expansion process under different rotation speeds, (a) $n = 1$ RPM; (b) $n = 500$ RPM; (c) $n = 1000$ RPM ($\delta = 1.2$, $\gamma = 0.027$, $\lambda = 0.5$, $\beta = 3.325$, $T_0 = 460$ K)

It is shown that there is a pressure drop at the beginning of the expansion, then the pressure rises quickly, and the expansion process goes on. This is because the evaporating rate is zero at the beginning of the cyclone section, which results in a rapid decrease of pressure and a big superheat of the water. Then, the flash evaporation occurs and results in a fast pressure recovery. It is also shown that pressure p in the cylinder would decrease more fast when the rotation speed is increased. The saturation pressure p_{sat} , corresponding to the temperature of the water in the cyclone, is bigger than the pressure p in the cylinder. This means that the water is in a superheated condition. And this superheat is larger for higher rotation speed. The actual water temperature T in the cyclone and the saturation temperature T_{sat} of water under the pressure in the cylinder are shown in Fig. 5.

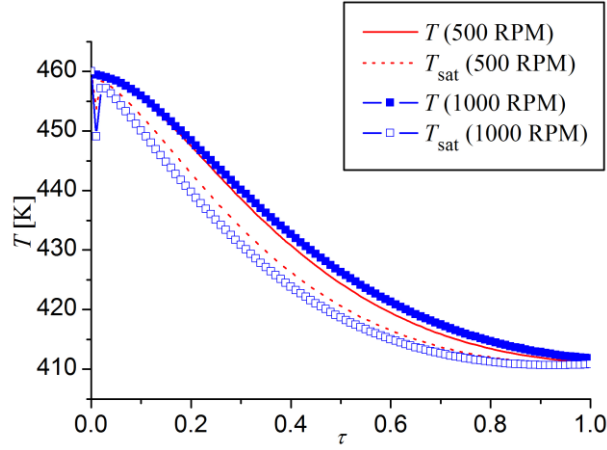


Fig. 5. Temperature evolution of water during the expansion process ($\delta = 1.2$, $\gamma = 0.027$, $\lambda = 0.5$, $\beta = 3.325$, $T_0 = 460$ K)

Figure 5 shows the decreasing temperature and the saturation temperature during the expansion process. At the beginning, the superheat is increased quickly, because the evaporating rate is zero. Then, during the following expansion process, the superheat is increased and later on decrease again.

4.2. Influence of the cyclone volume

In order to investigate the influence of the cyclone volume, the size of the cylinder and the injected water mass flow rate remain unchanged. When the volume of the cyclone is changed, both the ratios, δ and λ , of the cyclone volume to the initial volume of the water are changed.

As shown in Fig. 6, the efficiency of the expander will decrease when the cyclone volume is increased. A bigger cyclone volume means more evaporated vapor to fill during the expansion process, and it results in a lower pressure evolution profile during the expansion, as shown in Fig. 7. Thus, a higher cyclone volume will result in a lower efficiency.

Figure 7 also shows an enlarged pressure drop at the beginning of the expansion process with a larger volume ratio, δ . This is because the evaporating rate is slower at the beginning of the expansion process when the volume of the cyclone is larger.

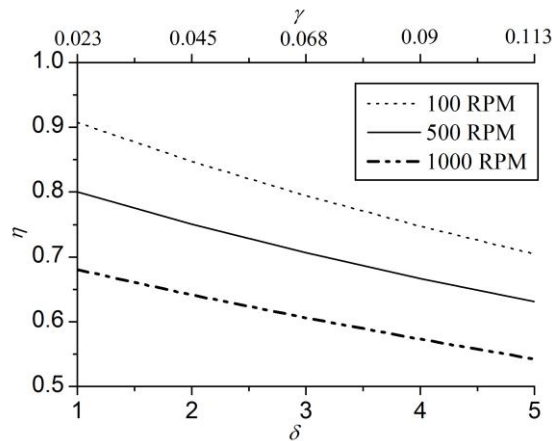


Fig. 6. Influence of cyclone volume on efficiency of the expander ($\lambda = 0.5$, $\beta = 3.325$, $T_0 = 460$ K)

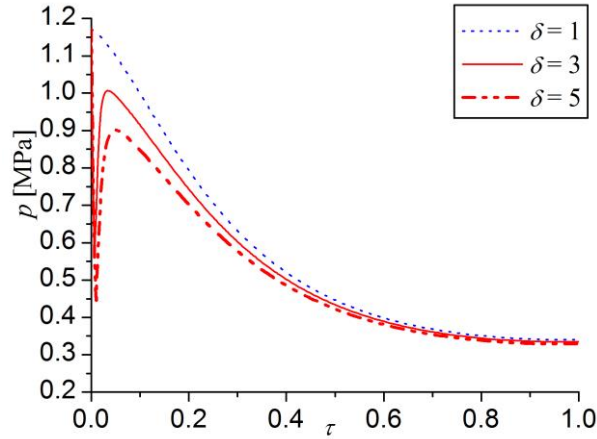


Fig. 7. Pressure evolution during the expansion process ($\lambda = 0.5$, $\beta = 3.325$, $n = 500$ RPM, $T_0 = 460$ K)

4.3. Influence of the injected mass

As shown in Fig. 8, efficiency is extremely high, when the injected mass is very low. However, the pressure ratio of the expander is large too. A larger pressure ratio will result in higher leakage and mechanic loss, and it will also increase the cost of the expander. The initial pressure is 1.17 MPa, which is set as the saturation pressure of water at 460 K. A higher pressure ratio also means low discharge pressure, even a vacuum. If the discharge pressure is set as the standard atmospheric pressure, its pressure ratio is 11.6 and the ratio β is 0.75. This has also been indicated by the 0.1 MPa line in Fig. 7. Thus, β is suggested as bigger than 0.75.

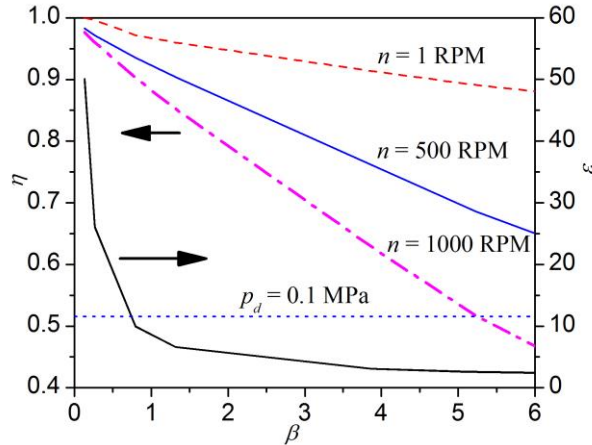


Fig. 8. Efficiency and pressure ratio of the expander with different β and rotation speeds ($\lambda = 0.5$, $\delta = 1.2$, $T_0 = 460$ K)

4.4. Influence of the injected water temperature

The efficiency of the expander decreases clearly with decreasing injected water temperature, as shown in Fig. 9(a). A low injected water temperature also results in low pressure evolution, and the pressure value will be below barometric pressure, as shown in Fig. 9(b). The negative pressure will increase the difficulty and cost for designing and manufacturing the expander. This means that refrigerants with lower boiling points are more appropriate than water for low temperature heat source.

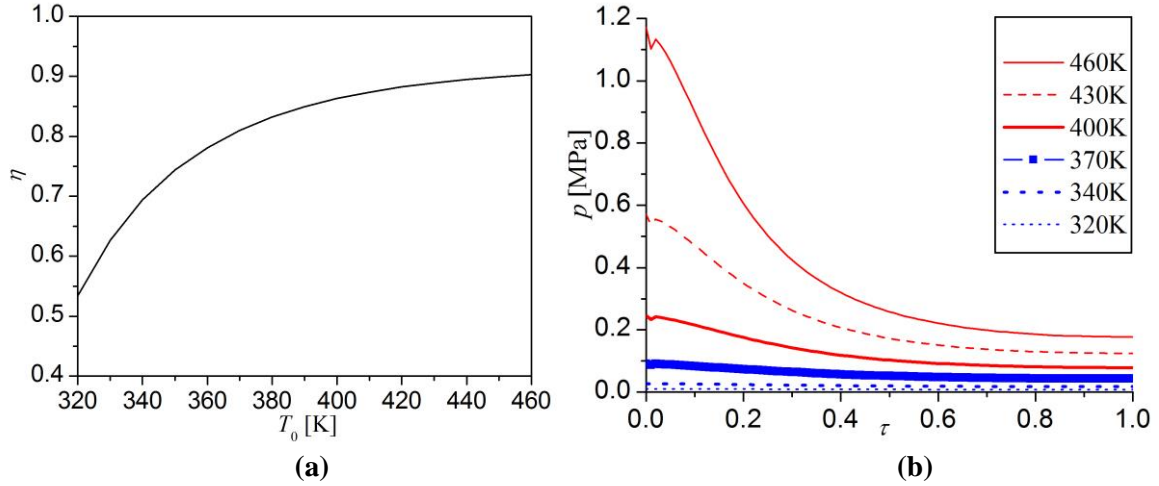


Fig. 9. Efficiency and pressure evolution of the expansion process with different injected water temperatures, (a) Isentropic efficiency of the expander in function of injected water temperature; (b) pressure evolution ($\lambda = 0.5$, $\delta = 1.2$, $\beta = 1.33$, $\gamma = 0.011$, $n = 500$ RPM)

4.5. Influence of shape of the cylinder

In Fig. 10, the pressure evolution profiles of the expansion process under different diameter/length ratios (λ) are presented. For a larger λ , more work is generated, which results in a higher efficiency. The reason for this is that the average speed of the piston is smaller for larger diameter/length ratio in a condition of constant cylinder volume. However, a too large diameter/length ratio is not good for a reciprocating expander, because the big piston would result in a large reciprocating mass.

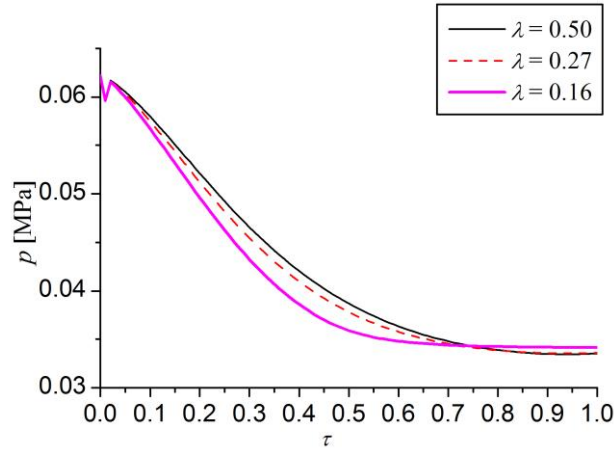


Fig. 10. Pressure evolution profiles of the expansion process under different diameter/length ratios ($\delta = 1.2$, $\beta = 1.33$, $\gamma = 0.011$, $n = 500$ RPM, $T_0 = 360$ K)

5. Conclusions

A simulation model of the two-phase expansion with water as the refrigerant in a reciprocating expander is developed in this paper. The approximate evaporating mass flow rate is introduced into the simulation model.

(1) Obtained results show that there is a sudden pressure drop at the beginning of the expansion process, and the pressure drop would be more large when the rotation speed is increased. Meanwhile, the superheat of the liquid is also increased rapidly.

(2) Higher cyclone volume, which is also called as clearance volume in a reciprocating expander, would decrease efficiency of the expander. From this perspective, a rotary expander is much more suitable for two-phase expansion due to its zero clearance volume.

(3) Efficiency is extremely high, when the injected mass is very low. However, pressure ratio of the expander is big too. For water, if the discharge pressure set as the standard atmospheric pressure, the injected water mass ratio, β , is suggested as bigger than 0.75. Thus, refrigerants with lower boiling points are suggested as working fluid of the two-phase expander.

Simulation results support the conclusion that higher evaporating rate would lead to higher efficiency of the two-phase expansion process. That means higher disturbing, larger number of bubble cores and bigger wall area of the cyclone would improve the two-phase expansion process. Based on this consideration, rotary expanders, such as the twin-screw expanders, are more suitable for two-phase expansion process than the reciprocating expanders.

Acknowledgment

This work was supported by the National Natural Science Foundation of China [grant number 51109174] and Shaanxi Province Industrial Science and Technology Project [grant number 2015GY089].

Nomenclature

a – coefficient, [–]	<i>Greek symbols</i>
A – area, [m ²]	τ – time ratio, [–]
c_p – isobaric heat capacity, [J/(kg·K)]	Δ – difference, [–]
d – diameter, [m]	ρ – density, [kg/m ³]
e – error, [–]	λ – length ratio, [–]
h – specific enthalpy, [J/kg]	δ – volume ratio, [–]
H – height, [m]	γ – volume ratio, [–]
L – length, [m]	β – volume ratio, [–]
m – flash evaporating rate, [kg/(m ³ ·s)]	μ – coefficient, [–]
M – mass, [kg]	η – efficiency, [%]
n – rotation speed of the expander, [r/min]	ε – pressure ratio, [–]
p – pressure, [Pa]	
P – power, [W]	<i>Subscripts</i>
r – latent heat, [J/kg]	c – cylinder
t – time, [s]	d – dead
T – temperature, [K]	dis – discharge
V – volume, [m ³]	ev – evaporated
W – work, [J]	i – injected
	is – isentropic

<i>Acronyms</i>	L – liquid
NEF – non-equilibrium function	mev – maximum evaporating rate
ORCs – Organic Rankine Cycles	sat – saturation
RPM – round per minute (engine speed)	th – thermal
TFC – Trilateral Flash Cycle	v – vapor

References

- [1] Pei, G., et al., Construction and dynamic test of a small-scale organic rankine cycle, *Energy*, 36 (2011), 5, pp. 3215-3223
- [2] Tahani, M., et al., A comprehensive study on waste heat recovery from internal combustion engines using organic Rankine cycle, *Thermal Science*, 17 (2013), 2, pp. 611-624
- [3] Barbazza, L., et al., Optimal design of compact organic Rankine cycle units for domestic solar applications, *Thermal Science*, 18 (2014), 3, pp. 811-822
- [4] Zhu, Q., et al., Performance analysis of organic Rankine cycles using different working fluids, *Thermal Science*, 19 (2015), 1, pp. 179-191
- [5] Kang, S.H., Design and preliminary tests of ORC (organic Rankine cycle) with two-stage radial turbine, *Energy*, 96 (2016), pp. 142-154
- [6] Ganesh, S.,T. Srinivas, Processes development for high temperature solar thermal Kalina power station, *Thermal Science*, 18 (2014), suppl.2, pp. 393-404
- [7] Modi, A.,F. Haglind, Performance analysis of a Kalina cycle for a central receiver solar thermal power plant with direct steam generation, *Applied Thermal Engineering*, 65 (2014), 1-2, pp. 201-208
- [8] Wang, E.,Z. Yu, A numerical analysis of a composition-adjustable Kalina cycle power plant for power generation from low-temperature geothermal sources, *Applied Energy*, 180 (2016), pp. 834-848
- [9] Cao, L., et al., Thermodynamic analysis of a Kalina-based combined cooling and power cycle driven by low-grade heat source, *Applied Thermal Engineering*, 111 (2017), pp. 8-19
- [10] Modi, A.,F. Haglind, Thermodynamic optimisation and analysis of four Kalina cycle layouts for high temperature applications, *Applied Thermal Engineering*, 76 (2015), pp. 196-205
- [11] Modi, A., et al., Thermoeconomic optimization of a Kalina cycle for a central receiver concentrating solar power plant, *Energy Conversion and Management*, 115 (2016), pp. 276-287
- [12] Smith I.K., Development of the trilateral flash cycle system Part 1: fundamental considerations, *Proceedings of the Institution of Mechanical Engineers Part a-Journal of Power and Energy*, 207 (1993), A3, pp. 179-194
- [13] Smith I.K., Dasilva R.P.M., Development of the trilateral flash cycle system Part 2: increasing power output with working fluid mixtures, *Proceedings of the Institution of Mechanical Engineers Part a-Journal of Power and Energy*, 208 (1994), A2, pp. 135-144
- [14] Ajimotokan, H.A.,I. Sher, Thermodynamic performance simulation and design optimisation of trilateral-cycle engines for waste heat recovery-to-power generation, *Applied Energy*, 154 (2015), pp. 26-34
- [15] Garcia, R.F., et al., Energy and entropy analysis of closed adiabatic expansion based trilateral cycles, *Energy Conversion and Management*, 119 (2016), pp. 49-59
- [16] Fischer, J., Comparison of trilateral cycles and organic Rankine cycles, *Energy*, 36 (2011), 10, pp. 6208-6219

- [17] Yari, M., et al., Exergoeconomic comparison of TLC (trilateral Rankine cycle), ORC (organic Rankine cycle) and Kalina cycle using a low grade heat source, *Energy*, 83 (2015), pp. 712-722
- [18] Lai, N.A.,J. Fischer, Efficiencies of power flash cycles, *Energy*, 44 (2012), 1, pp. 1017-1027
- [19] Smith I.K., et al., Development of the trilateral flash cycle system Part 3: the design of high-efficiency two-phase screw expanders, *Proceedings of the Institution of Mechanical Engineers Part a-Journal of Power and Energy*, 210 (1996), 1, pp. 75-93
- [20] Bao, J.,L. Zhao, A review of working fluid and expander selections for organic Rankine cycle, *Renewable and Sustainable Energy Reviews*, 24 (2013), pp. 325-342
- [21] Bianchi, G., et al., Development and analysis of a packaged Trilateral Flash Cycle system for low grade heat to power conversion applications, *Thermal Science and Engineering Progress*, 4 (2017), pp. 113-121
- [22] Kanno, H.,N. Shikazono, Modeling study on two-phase adiabatic expansion in a reciprocating expander, *International Journal of Heat and Mass Transfer*, 104 (2017), pp. 142-148
- [23] Bianchi, G., et al., Numerical modeling of a two-phase twin-screw expander for Trilateral Flash Cycle applications, *International Journal of Refrigeration*, 88 (2018), pp. 248-259
- [24] Kanno, H.,N. Shikazono, Experimental and modeling study on adiabatic two-phase expansion in a cylinder, *International Journal of Heat and Mass Transfer*, 86 (2015), pp. 755-763
- [25] Steffen, M., et al., Efficiency of a new Triangle Cycle with flash evaporation in a piston engine, *Energy*, 57 (2013), pp. 295-307
- [26] Miyatake O., et al., An experimental-study of spray flash evaporation, *Desalination*, 36 (1981), 2, pp. 113-128
- [27] Gopalakrishna S., et al., An experimental-study of flash evaporation from liquid pools, *Desalination*, 65 (1987), 1-3, pp. 139-151
- [28] Yan, J.J., et al., Experimental study on static/circulatory flash evaporation, *International Journal of Heat and Mass Transfer*, 53 (2010), 23-24, pp. 5528-5535
- [29] Saury, D., et al., Flash evaporation from a water pool: Influence of the liquid height and of the depressurization rate, *International Journal of Thermal Sciences*, 44 (2005), 10, pp. 953-965
- [30] Saury D., et al., Experimental study of flash evaporation of a water film, *International Journal of Heat and Mass Transfer*, 45 (2002), 16, pp. 3447-3457
- [31] Zhang, D., et al., Study on steam-carrying effect in static flash evaporation, *International Journal of Heat and Mass Transfer*, 55 (2012), 17-18, pp. 4487-4497
- [32] Zhao, B., et al., Experimental study on equilibrium waterfilm concentration in static flash evaporation of aqueous NaCl solution, *Desalination*, 353 (2014), pp. 109-117
- [33] Zhang, D., et al., Experimental study on static flash evaporation of aqueous NaCl solution, *International Journal of Heat and Mass Transfer*, 55 (2012), 23-24, pp. 7199-7206
- [34] Nist standard reference database 23: reference fluid thermodynamic and transport properties-refprop, Version 9.0. National Institute of Standards and Technology, Standard reference data program, Gaithersburg, Maryland, USA, 2010